Research Letter

ATP synthase: constrained stoichiometry of the transmembrane rotor

Daniel J. Müller[a,b,*], Norbert A. Dencher[c], Thomas Meier[d], Peter Dimroth[d], Kitaru Suda[b], Henning Stahlberg[b], Andreas Engel[b], Holger Seelert[c], Ulrich Matthey[d]

[a] *Max-Planck-Institute of Molecular Cell Biology and Genetics, D-01307 Dresden, Germany*
[b] *M.E. Müller-Institute for Structural Biology, Biozentrum, University of Basel, CH-4056 Basel, Switzerland*
[c] *Physical Biochemistry, Department of Chemistry, Darmstadt University of Technology, D-64287 Darmstadt, Germany*
[d] *Institute of Microbiology, Eidgenössische Technische Hochschule (ETH), CH-8092 Zurich, Switzerland*

Received 11 June 2001; accepted 26 June 2001

First published online 26 July 2001

Edited by Andreas Engel and Giorgio Semenza

Abstract Recent structural data suggest that the number of identical subunits (*c* or III) assembled into the cation-powered rotor of F_1F_0 ATP synthase depends on the biological origin. Atomic force microscopy allowed individual subunits of the cylindrical transmembrane rotors from spinach chloroplast and from *Ilyobacter tartaricus* ATP synthase to be directly visualized in their native-like environment. Occasionally, individual rotors exhibit structural gaps of the size of one or more subunits. Complete rotors and arch-shaped fragments of incomplete rotors revealed the same diameter within one ATP synthase species. These results suggest the rotor diameter and stoichiometry to be determined by the shape of the subunits and their nearest neighbor interactions.

Key words: Atomic force microscopy; ATP synthase; Structural assembly; Molecular interaction

1. Introduction

F_1F_0 ATP synthases are large multi-subunit membrane enzymes that convert the energy of an electrochemical cation (H^+ or Na^+) gradient into the biological energy currency ATP. Their membrane resident complex F_0 couples the transmembrane flow of cations to the rotation of a molecular stalk [1–4]. The rotating stalk drives sequential conformational changes in the three catalytic sites of the cytoplasmic F_1 complex, thereby catalysing synthesis and release of ATP. While the catalytic subcomplex $\alpha_3\beta_3\gamma$, as well as the subunits δ and ε of F_1, have been solved [5–10], the structure of the F_0 complex still awaits elucidation at atomic resolution.

The rotor of the cation-driven motor in F_0 is a ring of identical transmembrane α-helical hairpins, named subunit *c* in bacteria and mitochondria or subunit III in chloroplasts. While 10 identical subunits (c_{10}) compose the transmembrane rotor of yeast ATP synthase [11], the rotor of *Ilyobacter tartaricus* exhibits 11 subunits (c_{11}) [12], and the rotor of spinach chloroplast ATP synthase is assembled from 14 subunits (III_{14}) [13]. The mechanism determining the number of subunits forming the oligomeric rotor is essential, since its stoichiometry determines the gear between cation flow and ATP production [14,15]. Whereas the structure of the yeast rotor was solved to 4 Å by X-ray crystallography, single transmembrane rotors from proton-driven chloroplast and from sodium-driven *I. tartaricus* ATP synthase were imaged using atomic force microscopy (AFM). By comparison of complete and incomplete oligomers, we show the rotor diameter to be determined by interactions between neighboring subunits and their shape.

2. Materials and methods

2.1. Sample preparation

CF_0F_1 was isolated from spinach chloroplasts and pre-purified according to [27]. ATP synthase containing fractions were collected after rate–zonal centrifugation. CF_0F_1 obtained using this procedure and upon electroelution (see below) were active ATP synthases [28]. To isolate intact subunit III oligomers, sodium dodecyl sulfate (SDS) was added to CF_0F_1 obtained from the rate–zonal centrifugation. After this, the sample was loaded onto a glycerol gradient containing the detergent dodecyl maltoside. Material from this linear glycerol gradient containing the III_{14} oligomers was collected and reconstituted into lipid bilayers (phosphatidylcholine and phosphatidic acid from egg yolk) in the presence of dodecyl maltoside. The detergent was removed by treatment with BioBeads SM2 (Bio-Rad, Hercules, CA, USA). Alternatively, III_{14} oligomers of CF_0 were purified by blue native gel electrophoresis [29], omitting exposure to SDS. For the dissociation of CF_0F_1 into its subcomplexes CF_1 and CF_0, the gel contained 0.02% Coomassie blue G250. CF_0 was electroeluted from the gel and 2D arrays of the III_{14} oligomer were prepared as described above. Subunit III oligomers prepared by either one of the two different methods and investigation by AFM showed no structural differences (no data shown, see also [13]).

ATP synthase from *I. tartaricus* was purified as described [19]. c_{11} oligomers were purified from disrupted ATP synthase complexes by sucrose density gradient centrifugation to a final concentration of 0.8 mg/ml. For crystallization c_{11} oligomers solubilized in 2.4% β-octyl-glucoside were mixed with palmitoyl-oleoyl phosphatidylcholine at a lipid-to-protein ratio of 1.5 (w/w) and dialyzed in a temperature-controlled dialysis apparatus for 60 h against detergent-free buffer (200 mM NaCl, 10 mM Tris–HCl, pH 7.0).

2.2. AFM

The samples were diluted to a concentration of ~10 μg/ml in buffer solution and adsorbed to freshly cleaved mica [30]. Contact mode AFM topographs were recorded at room temperature after adjusting the electrolyte concentration of the buffer to allow electrostatically

*Corresponding author. Fax: (49)-351-210 1409.
E-mail address: daniel.mueller@mpi-cbg.de (D.J. Müller).

Abbreviations: AFM, atomic force microscopy; ATP, adenosine triphosphate; SDS, sodium dodecyl sulfate

0014-5793/01/$20.00
PII: S0014-5793(01)02708-9

balanced high-resolution imaging at a stylus loading force of <100 pN [16]. No differences between topographs recorded simultaneously in trace and in retrace direction were observed, indicating that the scanning process did not influence the appearance of the biological sample. Repeated imaging showed that the imaging conditions used did not produce incomplete rotors nor did it change the gap size of incomplete rotors. The AFM used was a Nanoscope III (Digital Instruments, Santa Barbara, CA, USA) equipped with a *J*-scanner (scan size 120 μm) and a fluid cell. Cantilevers (Olympus, Tokyo, Japan) had oxide-sharpened Si_3N_4 tips and a nominal spring constant of 0.09 N/m.

3. Results and discussion

3.1. Single-molecule imaging

III_{14} oligomers of spinach chloroplast F_0 and c_{11} oligomers of *I. tartaricus* F_0 were reconstituted into lipid bilayers [12,13] and imaged in buffer solution by AFM (Fig. 1). The densely packed arrangements of the cylindrical subunit III oligomers and subunit *c* oligomers are clearly seen in Fig. 1A,B, respectively. In both images, the two rotor ends are alternately exposed to the membrane surface. Wide rings of complete chloroplast rotors exhibit a mean outer diameter of 7.4 ± 0.3 nm, while the corresponding ends of bacterial rotors have an outer diameter of 5.7 ± 0.3 nm.

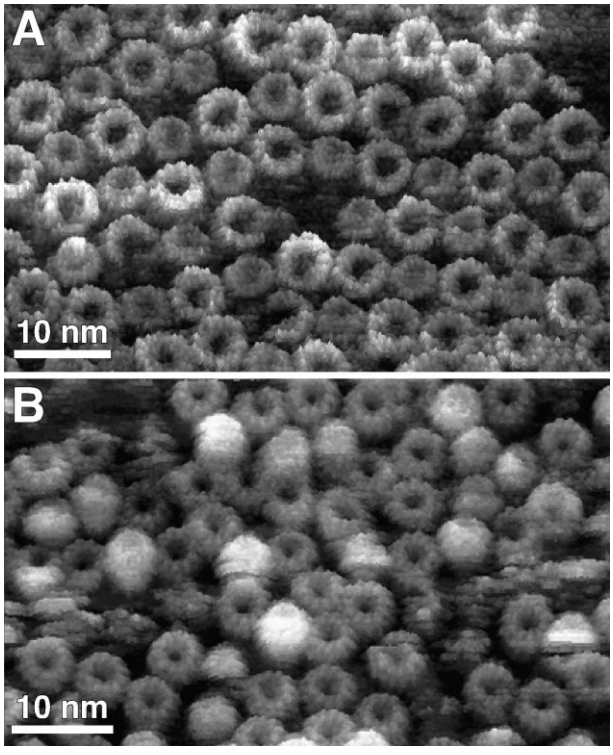

Fig. 1. AFM topographs of proton-driven rotors of spinach chloroplast ATP synthase (A) and of sodium-driven rotors of ATP synthase from *I. tartaricus* (B). Individual rotors expose one or the other of their ends. The subunits of the rotors can be easily distinguished on the unprocessed images. The chloroplast III_{14} rotor (A) exhibits a wide and a narrow end with diameters of 7.4 ± 0.3 nm and of 5.9 ± 0.3 nm, respectively. The two ends of the *I. tartaricus* c_{11} rotor (B) also have slightly different diameters, 5.7 ± 0.3 nm and 5.4 ± 0.3 nm, and protrude by different extends of the membrane surface. Both samples were prepared and imaged in buffer solution at room temperature using contact-mode AFM as recently described [12,13]. Reconstituted III oligomers of chloroplast ATP synthase, purified by two independent procedures, either with or without SDS, were used for the analysis shown in Fig. 2. The AFM topographs exhibit a vertical range of 2 nm and are displayed in a perspective view (5° tilt).

3.2. Individual incomplete rotors

Occasionally single rotors exhibited structural gaps of one or more missing subunits (Fig. 2). Images of single rotors reflected the individuality of their gaps. The percentage of incomplete rotors was about 2–3%. Consecutive imaging of the same rotors showed that the percentage of incomplete rotors and individuality of their gaps was not altered by the AFM imaging process (data not shown). As previously demonstrated, this routine control proved what was expected, since it has been repetitively demonstrated that AFM is capable of reproducibly imaging structural details of single proteins without distorting their native conformation [16–18]. Inspection of more than 1500 oligomers imaged in crystalline and non-crystalline areas revealed that each missing subunit leaves a structural gap of a precise size. Each subunit of the wide rotor ends exhibited an outer perimeter of 1.6 ± 0.1 nm and an inner perimeter of 0.8 ± 0.1 nm. Within the experimental error of 0.1 nm, both ATP synthase rotor subunits possess the same dimensions, although the mass of subunit III (8.0 kDa) [13] and *c* (8.7 kDa) [12] differ. However, all incomplete oligomers observed were arranged into circular structures. This implies that the III and *c* subunits exhibit an intrinsic curvature and interactions that allow their assembly into cylindrical rotors. To elucidate this phenomenon in more detail, we analyzed the diameter of incomplete oligomers, such as those displayed in Fig. 2. While the incomplete wide rings of the chloroplast rotor exhibited an average diameter of 7.3 ± 0.3 nm ($n = 136$), that of the incomplete bacterial rotor was found to be 5.6 ± 0.3 nm ($n = 168$). These diameters are identical to those of intact rotors within the experimental error.

3.3. Origin of incomplete rotors

To answer the question whether the incomplete rotors originate from the biochemical sample preparation, SDS gels of the samples investigated by AFM were produced (Fig. 3). Both preparations showed the complete subunit III_{14} (Fig. 3A) and c_{11} (Fig. 3B) oligomers to migrate as a single characteristic band [12,13], while a weakly staining band suggested monomeric subunits III in Fig. 3B and *c* in Fig. 3A. As shown previously, complete transmembrane rotors from chloroplast and from *I. tartaricus* ATP synthase form stable oligomeric assemblies, which only dissolve under harsh conditions, such as boiling in SDS solution [19]. This leads to the conclusion that a minority of subunits either exist in a monomeric form or that these subunits are assembled into less stable oligomers, which disassemble under conditions used for the SDS gel. This result may also suggest that not all subunits assemble into complete rings, in agreement with our structural observations.

3.4. Implications of incomplete rotors

Although above results do not allow to verify whether the incomplete ATP synthase rotors result from the biogenesis or from the biochemical preparation methods, they clearly show that the multimeric assembly of the subunits can form stable partial complexes in the lipid membrane. As demonstrated by topographs (Figs. 1 and 2), individual complete and incomplete rings can exhibit a slightly elliptical shape. This suggests

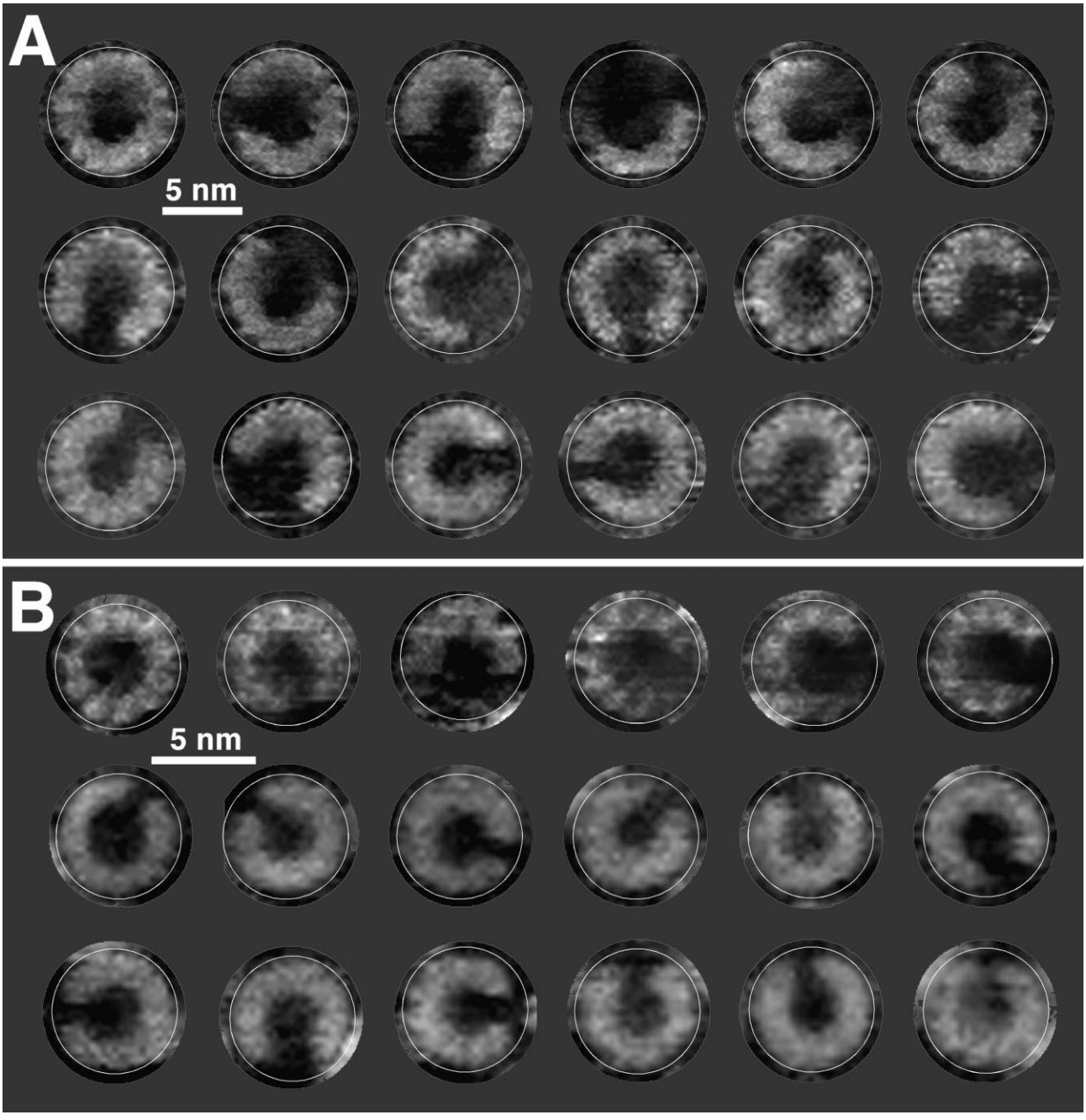

Fig. 2. Analysis of single ion-driven rotors of ATP synthase. A: Complete (top left) and incomplete chloroplast rotors. B: Complete (top left) and incomplete *I. tartaricus* rotors. Individual oligomeric rotors are missing one or several subunits III (A) or *c* (B). The wide rotor ends were selected for the analysis because they were imaged in greater detail. To measure the radius of curvature of the incomplete rotors, circles of different diameters were superimposed until the best fit was found at full-width–half-maximum of the protrusions. A circle exhibiting a diameter of 7.5 nm (A) and of 5.8 nm (B) was outlined on each rotor. The circle diameter of the rotors was found to be independent from the number of subunits missing. The incomplete chloroplast rotors had an average diameter of 7.3 ± 0.3 nm ($n = 136$) and those of *I. tartaricus* had an average diameter of 5.6 ± 0.3 nm ($n = 168$). Reconstituted III oligomers of chloroplast ATP synthase, purified by two independent procedures, either with or without SDS, were used for the analysis. Vertical range of the AFM topographs = 2 nm.

the rotors to be rather flexible structures that can be deformed by intermolecular interactions within the membrane. In spite of this, the analysis of defect rings imaged in more than 100 topographs demonstrate that the average ring diameter and its standard deviation remained unaffected by the completeness of the rotor. Additionally, no dependence of the rotor diameter on its crystalline or non-crystalline assembly into the membrane was observed. The occasionally detected deformation of single complete and incomplete rotors ($< 5\%$) suggest that the rotor subunits energetically favor to assemble into a cylindrical shape.

The partial rings displayed in Fig. 2 also indicate that the diameter of the membrane-embedded ATP synthase rotor is independent of the number of subunits assembled into circular-shaped rotor fragments. Therefore, the rotor diameter is constrained by the subunit itself, which possess an intrinsic

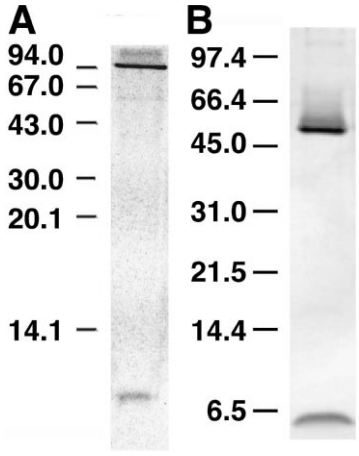

Fig. 3. Analysis by SDS gel electrophoresis and silver staining of the cation-driven ATP synthase rotors investigated by AFM. Lanes (A) and (B) show preparations of subunit III_{14} oligomers of chloroplast ATP synthase and subunit c_{11} oligomers of *I. tartaricus* ATP synthase, respectively, upon reconstitution in lipid bilayers. Sample (A) was analyzed using a 14% SDS gel [31], while sample (B) was visualized on a 13.4% SDS gel [32]. Molecular masses (kDa) of protein standards are indicated on the left side of each lane. Both samples were treated at room temperature. In contrast to the chloroplast sample, the c_{11} oligomer and the c_1 monomer exhibit an abnormal migration behavior as compared to the molecular mass protein standards.

curvature defining the diameter and, hence, the structural stoichiometry of the rotor. Both the diameter of incomplete rotors and the consistent size of structural gaps suggest that no significant conformational change of the rotor subunit is requested for their assembly.

3.5. Conclusions

In current models of the ATP synthase, the cation-to-ATP stoichiometry of the ATP synthesis is directly linked to the subunit stoichiometry of the cation-powered rotor [14,20]. Recent structural data suggest that the subunit stoichiometry depends on the biological species from which the ATP synthase originates [11–13]. Topographs of rotors from two different ATP synthases now show that the diameter of incomplete rotors missing several subunits is equal to that of intact rotors (Fig. 2). This allows following conclusions to be drawn: The diameter, and thereby the subunit, stoichiometry of the electrochemically driven rotor appears to be constant for the respective ATP synthases investigated. The diameter of these rotors appears to be constrained by intrinsic properties of the transmembrane subunits (III or *c*) forming the oligomer. This suggests the cation-to-ATP stoichiometry of ATP synthesis to be a constant within the same biological species [14]. In contrast, Schemidt et al. [21] suggest a dependence of the subunit stoichiometry on the metabolic state of *Escherichia coli*.

3.6. Relevance to other proteins

Observation of single proteins in their physiologically relevant environment at submolecular resolution is an extremely powerful approach, which in this study, yielded insights about the assembly of subunits into a homo-oligomer. Both the size and stoichiometry of the cation-powered ATP synthase rotor are determined by intrinsic properties of its subunits. This finding may also be of relevance for the assembly of other homo-oligomers [22–24]. Extended applications of single-molecule microscopy should, in the future, allow even more detailed investigations of membrane protein assembly and function [25,26].

Acknowledgements: The authors thank Drs. K. Altendorf, J. Howard, W. Junge, W. Kühlbrandt, S. Müller and S. Scheuring for helpful discussions.

References

[1] Sabbert, D., Engelbrecht, S. and Junge, W. (1996) Nature 381, 623–625.
[2] Noji, H., Yasuda, R., Yoshida, M. and Kinosita, K. (1997) Nature 386, 299–302.
[3] Sambongi, Y. et al. (1999) Science 286, 1722–1724.
[4] Pänke, O., Gumbiowski, K., Junge, W. and Engelbrecht, S. (2000) FEBS Lett. 472, 34–38.
[5] Abrahams, J.P., Leslie, A.G.W., Lutter, R. and Walker, J.E. (1994) Nature 370, 621–628.
[6] Bianchet, M.A., Hullihen, J., Pedersen, P.L. and Amzel, L.M. (1998) Proc. Natl. Acad. Sci. USA 95, 11065–11070.
[7] Wilkens, S., Dahlquist, F.W., McIntosh, L.P., Donaldson, L.W. and Capaldi, R.A. (1995) Nat. Struct. Biol. 2, 961–967.
[8] Wilkens, S., Dunn, S.D., Chandler, J., Dahlquist, F.W. and Capaldi, R.A. (1997) Nat. Struct. Biol. 4, 198–201.
[9] Gibbons, C., Montgomery, M.G., Leslie, A.G.W. and Walker, J.E. (2000) Nat. Struct. Biol. 7, 1055–1061.
[10] Rodgers, A.J.W. and Wilce, M.C.J. (2000) Nat. Struct. Biol. 7, 1051–1054.
[11] Stock, D., Leslie, A.G. and Walker, J.E. (1999) Science 286, 1700–1705.
[12] Stahlberg, H., Müller, D.J., Suda, K., Fotiadis, D., Engel, A., Matthey, U., Meier, T. and Dimroth, P. (2001) EMBO Rep. 21, 1–5.
[13] Seelert, H., Poetsch, A., Dencher, N.A., Engel, A., Stahlberg, H. and Müller, D.J. (2000) Nature 405, 418–419.
[14] Ferguson, S.J. (2000) Curr. Biol. 10, R804–R808.
[15] Stock, D., Gibbons, C., Arechaga, I., Leslie, A.G. and Walker, J.E. (2000) Curr. Opin. Struct. Biol. 10, 672–679.
[16] Müller, D.J., Fotiadis, D., Scheuring, S., Müller, S.A. and Engel, A. (1999) Biophys. J. 76, 1101–1111.
[17] Müller, D.J., Sass, H.-J., Müller, S., Büldt, G. and Engel, A. (1999) J. Mol. Biol. 285, 1903–1909.
[18] Heymann, J.B., Müller, D.J., Landau, E., Rosenbusch, J., Pebay-Peroulla, E., Büldt, G. and Engel, A. (1999) J. Struct. Biol. 128, 243–249.
[19] Neumann, S., Matthey, U., Kaim, G. and Dimroth, P. (1998) J. Bacteriol. 180, 3312–3316.
[20] Junge, W. (1999) Proc. Natl. Acad. Sci. USA 96, 4735–4737.
[21] Schemidt, R.A., Qu, J., Williams, J.R. and Brusilow, W.S. (1998) J. Bacteriol. 180, 3205–3208.
[22] Kühlbrandt, W., Wang, D.N. and Fujiyoshi, Y. (1994) Nature 367, 614–621.
[23] McDermott, G., Prince, S.M., Freer, A.A., Hawthornthwaite-Lawless, A.M., Papiz, M.Z., Gogdell, R.J. and Isaacs, N.W. (1995) Nature 374, 517–521.
[24] Koepke, J., Hu, X., Muenke, C., Schulten, K. and Michel, H. (1996) Structure 4, 581–597.
[25] Möller, C., Büldt, G., Dencher, N., Engel, A. and Müller, D.J. (2000) J. Mol. Biol. 301, 869–879.
[26] Engel, A. and Müller, D.J. (2000) Nat. Struct. Biol. 7, 715–718.
[27] Seelert, H., Poetsch, A., Rohlfs, M. and Dencher, N.A. (2000) Biochem. J. 346, 41–44.
[28] Poetsch, A., Neff, D., Seelert, H., Schagger, H. and Dencher, N.A. (2000) Biochim. Biophys. Acta 1466, 339–349.
[29] Neff, D. and Dencher, N.A. (1999) Biochem. Biophys. Res. Commun. 259, 569–575.
[30] Müller, D.J., Amrein, M. and Engel, A. (1997) J. Struct. Biol. 119, 172–188.
[31] Laemmli, U.K. (1970) Nature 227, 680–685.
[32] Schägger, H. and Jagow, G. (1987) Anal. Biochem. 166, 368–379.